Demonstration of Radiation Symmetry Control for Inertial Confinement Fusion in Double *Z*-Pinch Hohlraums

R. A. Vesey,[1,*] M. E. Cuneo,[1] G. R. Bennett,[2] J. L. Porter, Jr.,[1] R. G. Adams,[1] R. A. Aragon,[1] P. K. Rambo,[1] L. E. Ruggles,[1] W. W. Simpson,[1] and I. C. Smith[1]

[1]*Sandia National Laboratories, P.O. Box 5800, Albuquerque, New Mexico 87185-1186*
[2]*Ktech, Corp., 2201 Buena Vista SE, Suite 400, Albuquerque, New Mexico 87106-4265*

(Received 10 June 2002; published 23 January 2003)

Simulations of a double *Z*-pinch hohlraum, relevant to the high-yield inertial-confinement-fusion concept, predict that through geometry design the time-integrated P_2 Legendre mode drive asymmetry can be systematically controlled from positive to negative coefficient values. Studying capsule elongation, recent experiments on *Z* confirm such control by varying the secondary hohlraum length. Since the experimental trend and optimum length are correctly modeled, confidence is gained in the simulation tools; the same tools predict capsule drive uniformity sufficient for high-yield fusion ignition.

DOI: 10.1103/PhysRevLett.90.035005 PACS numbers: 52.59.Qy, 52.57.Fg, 52.58.Lq

Indirect-drive inertial confinement fusion (ICF), which seeks to compress fuel (typically deuterium-tritium) in a soft x-ray driven imploding capsule, places strict requirements on the thermal x-ray source with regard to pulse shaping, radiation symmetry, and fuel preheat [1]. In central hot-spot ignition ICF, the creation of a high-temperature (> 10 keV) central hot-spot with sufficient areal density (> 0.3 g/cm^2) relies on the precisely timed merger of radially convergent shocks at the center of the capsule, which ignites the fusion burn that then propagates into the surrounding high-density fuel layer. Variations of the thermal x-ray intensity on different parts of the capsule result in a nonspherical fuel implosion and can lead to failure in reaching the hot-spot conditions necessary for ignition. Thus, the symmetry of the thermal x-ray drive is a crucial issue: for example, ignition capsules for laser indirect-drive designs typically require $<1\%$–2% overall fluence asymmetry [2]. Because of this, a large fraction of the effort in the laser ICF community has been devoted to computational and experimental understanding of techniques for radiation symmetry control in laser-driven hohlraums. The initial steps toward experimentally validated symmetry control for *Z*-pinch ICF are described in this Letter.

Z pinches formed by the implosion of wire arrays have recently emerged as very efficient sources of thermal x rays [3] that may meet the requirements of a source for indirect-drive ICF, particularly suited to high fusion yield (> 400 MJ). One approach is the high-yield concept proposed by Hammer *et al.* [4], which uses a *Z*-pinch driven primary hohlraum at each end of a central coaxial secondary hohlraum containing the ICF capsule. Experiments on the *Z* accelerator [5] at Sandia National Laboratories have measured the pinch power, primary hohlraum radiation temperatures, and primary-secondary hohlraum coupling efficiency for configurations relevant to this concept [6–8] and have demonstrated a single-sided power feed, double-pinch load [8] for radiation symmetry experiments on *Z*. Figure 1 illustrates the features of the hohlraum geometry relevant for the design calculations and experimental data described in this Letter. Double-pinch experiments on *Z* have *Z*-pinch x-ray output energies of 0.8–1.3 MJ [9] and capsule drive temperatures of 70 eV, which scale to 16 MJ and 220 eV for the high-yield concept [4].

We have used viewfactor and radiation-hydrodynamics (RHD) models to design hohlraums that optimize the capsule radiation symmetry for near-term experiments and for high-yield targets [10,11]. Self-backlit foam ball burnthrough experiments have provided partial validation of these techniques, demonstrating gross

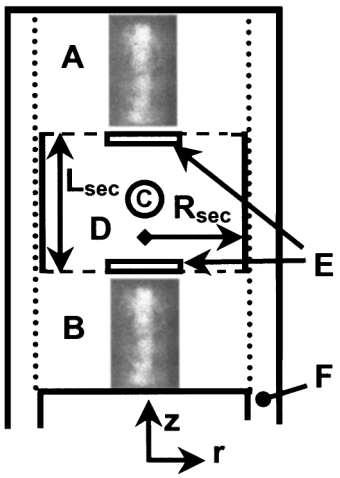

FIG. 1. Schematic of single-power-feed double pinch hohlraum geometry used in *Z* experiments: (*A*) upper primary hohlraum containing upper *Z* pinch (initial wire location shown as dotted line, stagnated pinch image shown); (*B*) lower primary hohlraum containing lower *Z* pinch; (*C*) implosion capsule; (*D*) secondary hohlraum; (*E*) on-axis shine shields, each of radius R_{shld}, at the center of a radial spoke array; (*F*) anode-cathode gap in power feed.

modifications of radiation symmetry in single-pinch hohlraums [12] and showing flux asymmetry levels lower than 15% maximum-to-minimum in double-pinch hohlraums [11,12]. Recently, an advanced double-pinch wire-array load for Z has been developed that provides balanced upper and lower pinch x-ray power histories such that measurements of upper and lower primary hohlraum wall emission temperatures agree within instrumental error bars [9]. For symmetry diagnosis, we are now using the Z-Beamlet Laser (ZBL) [13] to create high-energy x rays for point-projection backlighting of capsule implosions in double-pinch hohlraums. These images enable measurements of capsule in-flight distortions at the percent level [14] and allow fine-tuning of the radiation symmetry experimentally as well as providing a stringent test of our modeling techniques.

In this Letter, we describe the first demonstration of diagnosed, predictable radiation symmetry control in capsule implosions at the sub-10% level with a Z-pinch-driven hohlraum. We demonstrate that by varying the geometry of the hohlraum containing the capsule, the elongation of the backlit imploding capsule can be systematically controlled, in agreement with simulation results. [Elongation is defined as the ratio of the capsule diameter at the equator (from horizontal transmission profiles) to the capsule diameter at its poles (from vertical transmission profiles).] Symmetry control by hohlraum geometry design for Z pinches is directly analogous to varying the laser beam pointing, varying the hohlraum length, and axial shields that have all been successfully employed to control radiation symmetry in laser-driven hohlraums [1,15]. These results indicate that the double-pinch source reproducibility, hohlraum coupling energetics, symmetry diagnostics, and theoretical understanding of radiation transport and symmetry are nearing the goal of demonstrating radiation symmetry levels on Z that scale to high-yield hohlraum requirements.

In contrast to laser-driven hohlraums in which symmetry control is possible by properly positioning and programming the power in each of many laser beams injected into the hohlraum [1], the double-pinch hohlraums considered here contain just two extended plasma x-ray sources, the Z pinches themselves. A key result of earlier theoretical work [4,10] is that the level of radiation asymmetry at the capsule can be minimized by properly choosing the geometry of the secondary hohlraum (the hohlraum containing the capsule). This can be accomplished by simply varying the length of a cylindrical secondary hohlraum (as demonstrated in this Letter), by varying the secondary hohlraum radius and the radius of the on-axis shine shield at each entrance to the secondary, and by allowing a noncylindrical hohlraum shape to fine-tune the symmetry. We have developed the two-dimensional (axisymmetric), time-dependent viewfactor code OPTSEC [11] to model the effects of hohlraum geometry on capsule symmetry and to design the experiments summarized here. These OPTSEC calculations include the time-dependent Z-pinch source power as well as time-dependent wall albedo based on tabulated results from one-dimensional LASNEX [16] RHD simulations. The calculated time-dependent primary and secondary hohlraum emission temperatures have been benchmarked to the $\pm 5\%$ level against hohlraum energetics data [8,9]. OPTSEC can also be run in an optimization mode, varying hohlraum geometric variables and measuring the results against a set of design goals (e.g., minimum asymmetry) and constraints (e.g., hohlraum size, capsule stand-off, etc.).

Figure 2 shows the results of OPTSEC scoping calculations for a capsule in a double-pinch hohlraum, driven with a peak lower (upper) pinch power of 40 TW (38 TW) inferred from an earlier experiment [9]. Results are shown for various choices of secondary hohlraum radius R_{sec} and secondary hohlraum length L_{sec} for fixed primary hohlraum radius (13 mm) and shield radius (3.2 mm). The dominant effect of L_{sec} is on the P_2 Legendre mode, the extreme values of which occur at the poles (0° and 180°) and the equator (90°). Shorter-than-optimum secondary hohlraums lead to an equator-hot (negative P_2) fluence at the capsule, while longer-than-optimum hohlraums lead to a pole-hot (positive P_2) fluence. Because the capsule is shielded from direct x-ray flux emitted by the stagnated Z pinches, 75%–80% of the fluence is emitted by structures within the secondary hohlraum (cylindrical wall, on-axis shine shields), with the remaining 20%–25% contributed by primary hohlraum structures. The main effects of varying L_{sec} are to modify the generally pole-hot contribution from the primary hohlraum and to modify the generally equator-hot distribution from the cylindrical secondary wall, with the largest relative modification occurring at the capsule equator. At the optimum length, the superposition of primary hohlraum and secondary hohlraum

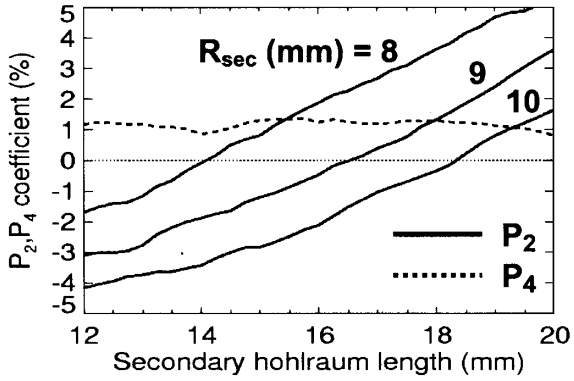

FIG. 2. OPTSEC viewfactor results for time-integrated P_2 (solid line) and P_4 (dashed line) vs secondary hohlraum length (L_{sec}) for various hohlraum radii (R_{sec}). Because P_4 does not vary significantly with R_{sec} alone, an average value is plotted.

wall radiation fluence reaching the capsule is such that polar angle variations are minimized.

For the Z experiments described here, wire-array hardware requirements constrained the secondary hohlraum radius R_{sec} to be 9.238 mm. Furthermore, the primary hohlraum radius (13 mm) and length (10 mm) were fixed. Preshot OPTSEC calculations indicated that for $R_{sec} = 9.2$ mm, a secondary hohlraum length $L_{sec} = 15.6$ mm and shine shield $R_{shld} = 3.25$ mm would provide minimum even Legendre mode asymmetry. To investigate the predicted dependence of even mode symmetry on secondary hohlraum length, multiple experiments at $L_{sec} = 13.0$, 15.6, and 17.4 mm ($L_{sec}/R_{sec} = 1.41$ to 1.88) were conducted during the same shot series. With ~40 TW peak power and ~0.4 MJ x-ray output per pinch, the expected capsule drive temperature peaks at 65–75 eV. Point-projection backlighting (6.7 keV, 600 ps pulse) of 2.15-mm initial diameter capsules during their implosion provide x-ray images with ~100 μm resolution. (Experimental details can be found in Ref. [14].)

For a direct comparison of theory and experiment, postshot calculations used the upper and lower primary hohlraum emission temperature histories (as measured by transmission grating spectrometers [8,9]). OPTSEC was iterated until its prescribed upper and lower Z-pinch power histories reproduced the measured hohlraum temperature histories. The OPTSEC time-dependent capsule radiation asymmetry was then applied as a source boundary condition to a separate two-dimensional LASNEX RHD simulation of the capsule implosion. Finally, the LASNEX capsule simulation was postprocessed, modeling the backlighter pulse-length (600 ps FWHM) and photon energy (6.7 keV) to produce synthetic backlit capsule images for comparison with the data. Figure 3 summarizes the results of the hohlraum length scan, with one backlit capsule image from each length (13.0, 15.6, and 17.4 mm). Each experimental image is accompanied by a simulation result at comparable convergence ratio (C_r), where C_r is defined as the ratio of the initial outer capsule radius to the radius of a sphere having the same enclosed volume as the ellipsoidal shell. The essential systematic trend from equator-hot (prolate image) through balanced (qualitatively spherical image) to pole-hot (oblate image) predicted by the calculations agrees with the experimental images. Given the simplicity of the model, the overall agreement with the experimental trend is encouraging, in particular, the agreement with the optimum hohlraum length. Z-pinch source distribution and motion [17], hohlraum wall motion, anode-cathode gap closure, non-Lambertian pinch emission, and time-varying nonuniform spoke transmission are some effects not contained in the piecewise calculations that could potentially influence P_2 at the few percent level. We speculate that the vertical absorption features in the top two of the three experimental images are due to hohlraum aperture blowoff plasma, ablated by the secondary hohlraum radiation

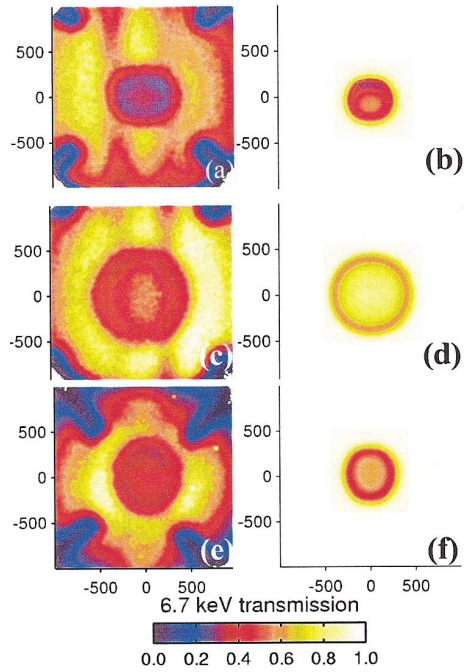

FIG. 3 (color). Experimental (left) and piecewise simulation (right) x-ray images for three secondary hohlraum lengths: (a),(b) 17.4 mm [$C_r \approx 6.4$], (c),(d) 15.6 mm [$C_r \approx 2.7$], (e),(f) 13.0 mm [$C_r \approx 4.1$]. Spatial dimensions are in microns at the target.

field, and assembled into vertical columns by the preferentially axial current flow on the outside of the secondary wall. This hypothesis is supported by the mitigation of these features when Mylar burnthrough foils were attached to each of the viewing apertures (bottom experimental image and two other shots at the 13 mm hohlraum length).

The piecewise viewfactor-RHD simulations described above are complemented by 2D axisymmetric LASNEX RHD hohlraum simulations [11], which include radially moving x-ray sources with prescribed output power histories to mock up the Z pinches, Lagrangian meshing (with discrete rezoning) of the hohlraum walls to consistently model wall motion and albedo, a multigroup radiation treatment, and capsule ablation/implosion physics. As in the piecewise calculations, we require calculated and measured primary hohlraum temperatures to agree as a figure of merit and generate synthetic backlit capsule images. Figure 4 summarizes the capsule elongation versus convergence ratio results for the images shown in Fig. 3 plus others obtained in this experimental series, compared with the trends in the 2D hohlraum simulation results. Experimental data with large asymmetric error bars represent the uncertainties due to the vertical absorption features [e.g.. Fig. 3(a)]. Simulations indicate that as the capsule implodes beyond $C_r = 7$–10, the optical depth for 6.7 keV backlighter x rays through the capsule center becomes high enough that a limb cannot be unambiguously identified. For cases in which a discernible limb is

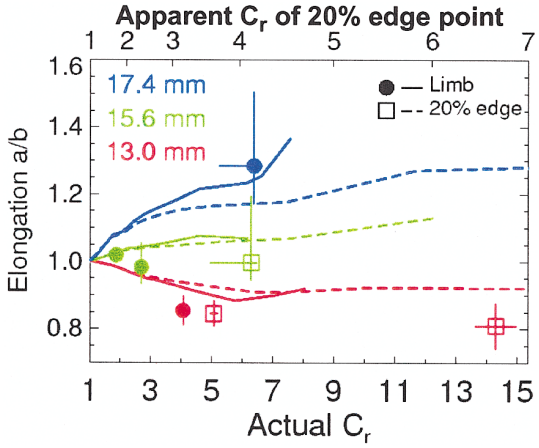

FIG. 4 (color). 2D hohlraum simulation results for backlit capsule elongation vs convergence ratio compared to experimental results. Simulation curves (solid and dotted lines) and data points are color coded according to secondary hohlraum length (13.0, 15.6, and 17.4 mm).

present (e.g., Fig. 3 images), the point of minimum transmission is used to define the shell radius. For profiles containing no discernible limb, a point at 20% of the difference between the minimum and maximum transmission is used. We use the simulations to relate the actual C_r (which agrees with the C_r obtained from the synthetic backlit images with a discernible limb) to the C_r obtained using the 20% edge radius. This relationship is shown using the upper and lower x axes in Fig. 4. (The 20% edge radius invariably underestimates C_r because it corresponds to a point in the capsule ablation plasma.) Filled-circle data points are to be compared with the solid simulation curves (limb elongation), while open-square data points are to be compared with the dashed simulation curves (20% edge elongation). The 2D hohlraum simulations corroborate the qualitative trend predicted by the piecewise calculations and yield excellent overall agreement with the data. While the implosion capsule used in these experiments is sufficient to distinguish asymmetry levels at the three hohlraum lengths used, more sensitive symmetry diagnostics such as high-aspect-ratio thin shells [18] may be necessary to measure pole-equator asymmetry at the 1% level to distinguish among models of Z-pinch source characteristics and anode-cathode gap closure.

In conclusion, polar radiation symmetry measurements at effective capsule drive temperatures of 70 ± 5 eV in a single power feed analog of the double-pinch high-yield hohlraum concept have demonstrated systematic control of even mode asymmetry at the sub-10% level in fluence. As calculated by piecewise viewfactor-radiation-hydrodynamics methods as well as 2D hohlraum simulations, the drive asymmetry on the capsule was experimentally varied from equator-hot, through balanced equator-to-pole, to pole-hot conditions by increasing the secondary hohlraum length-to-radius ratio from 1.4 to 1.9. Future experiments will seek to refine the experimental determination of the optimum hohlraum length for fixed hohlraum radius, precisely measure distorted shell Legendre mode coefficients at various C_r values, and test more fully optimized hohlraum geometries that may provide asymmetry levels that scale to high-yield requirements [9].

We gratefully acknowledge the Z and ZBL operations teams for technical support, support from T. Mehlhorn (Sandia), and useful discussions with J. Hammer, O. Landen (Livermore), and S. Slutz (Sandia). Sandia is a multiprogram laboratory operated by Sandia Corporation, a Lockheed Martin Company, for the U.S. Department of Energy under Contract No. DE-AC04-94AL85000.

*Electronic address: ravesey@sandia.gov

[1] J. Lindl, *Inertial Confinement Fusion: The Quest for Ignition and Energy Gain Using Indirect-Drive* (Springer-Verlag, New York, 1998).
[2] S. W. Haan *et al.*, Phys. Plasmas **2**, 2480 (1995).
[3] T. W. L. Sanford *et al.*, Phys. Rev. Lett. **77**, 5063 (1996); C. Deeney *et al.*, Phys. Rev. E **56**, 5945 (1997).
[4] J. H. Hammer *et al.*, Phys. Plasmas **6**, 2129 (1999).
[5] R. B. Spielman *et al.*, Phys. Plasmas **5**, 2105 (1998).
[6] J. L. Porter, Jr., Bull. Am. Phys. Soc. **42**, 1948 (1997); K. L. Baker *et al.*, Appl. Phys. Lett. **75**, 775 (1999).
[7] M. E. Cuneo *et al.*, Bull. Am. Phys. Soc. **44**, 40 (1999).
[8] M. E. Cuneo *et al.*, Phys. Plasmas **8**, 2257 (2001).
[9] M. E. Cuneo *et al.*, Phys. Rev. Lett. **88**, 215004 (2002).
[10] R. A. Vesey *et al.*, Bull. Am. Phys. Soc. **43**, 1903 (1998); **44**, 227 (1999); **45**, 360 (2000).
[11] R. A. Vesey *et al.*, in *Inertial Fusion Sciences and Applications 2001*, edited by K. A. Tanaka, D. D. Meyerhofer, and J. Meyer-ter-Vehn (Elsevier, Paris, 2002), p. 681.
[12] D. L. Hanson *et al.*, Phys. Plasmas **9**, 2173 (2002).
[13] G. R. Bennett *et al.*, Rev. Sci. Instrum. **72**, 657 (2001).
[14] G. R. Bennett *et al.*, Phys. Rev. Lett. (to be published).
[15] L. J. Suter *et al.*, Phys. Rev. Lett. **73**, 2328 (1994); T. J. Murphy and P. A. Amendt, ICF Q. Rep. **4**, 101 (1994) (National Technical Information Services Document No. DE95011970); O. L. Landen *et al.*, Phys. Plasmas **6**, 2137 (1999).
[16] G. B. Zimmerman and W. L. Kruer, Comments Plasma Phys. Controlled Fusion **2**, 51 (1975).
[17] M. E. Cuneo *et al.*, Bull. Am. Phys. Soc. **46**, 234 (2001).
[18] S. M. Pollaine *et al.*, Phys. Plasmas **8**, 2357 (2001); P. Amendt *et al.*, Phys. Plasmas **8**, 2908 (2001).